AJNR

DSA Quantitative Analysis and Predictive Modeling of Obliteration in Cerebral AVM following Stereotactic Radiosurgery

Mohamed Sobhi Jabal, Marwa A. Mohammed, Cody L. Nesvick, Hassan Kobeissi, Christopher S. Graffeo, Bruce E. Pollock and Waleed Brinjikji

AJNR Am J Neuroradiol 2024, 45 (10) 1521-1527
doi: https://doi.org/10.3174/ajnr.A8351
http://www.ajnr.org/content/45/10/1521

DSA Quantitative Analysis and Predictive Modeling of Obliteration in Cerebral AVM following Stereotactic Radiosurgery

Mohamed Sobhi Jabal, Marwa A. Mohammed, Cody L. Nesvick, Hassan Kobeissi, Christopher S. Graffeo, Bruce E. Pollock, and Waleed Brinjikji

ABSTRACT

BACKGROUND AND PURPOSE: Stereotactic radiosurgery is a key treatment modality for cerebral AVMs, particularly for small lesions and those located in eloquent brain regions. Predicting obliteration remains challenging due to evolving treatment paradigms and complex AVM presentations. With digital subtraction angiography (DSA) being the gold standard for outcome evaluation, radiomic approaches offer potential for more objective and detailed analysis. We aimed to develop machine learning modeling using DSA quantitative features for post-SRS obliteration prediction.

MATERIALS AND METHODS: A prospective registry of patients with cerebral AVMs was screened to include patients with digital prestereotactic radiosurgery DSA. Anterior-posterior and lateral views were retrieved and manually segmented. Quantitative features were computed from the lesion ROI. Following feature selection, machine learning models were developed to predict unsuccessful 2-year total obliteration using processed radiomics features in comparison with clinical and radiosurgical features. When we evaluated through area under the receiver operating characteristic curve (AUROC), accuracy, area under the precision-recall curve F1, recall, and precision, the best performing model predictions on the test set were interpreted using the Shapley additive explanations approach.

RESULTS: DSA images of 100 included patients were retrieved and analyzed. The best-performing clinical radiosurgical model was a gradient boosting classifier with an AUROC of 68% and a recall of 67%. When we used radiomics variables as input, the AdaBoost classifier had the best evaluation metrics with an AUROC of 79% and a recall of 75%. The most important clinico-radiosurgical features, ranked by model contribution, were lesion volume, patient age, treatment dose rate, the presence of seizure at presentation, and prior resection. The most important ranked radiomics features were the following: gray-level size zone matrix, gray-level nonuniformity, kurtosis, sphericity, skewness, and gray-level dependence matrix dependence nonuniformity.

CONCLUSIONS: The combination of radiomics with machine learning is a promising approach for predicting cerebral AVM obliteration status following stereotactic radiosurgery. DSA could enhance prognostication of stereotactic radiosurgery–treated AVMs due to its high spatial resolution. Model interpretation is essential for building transparent models and establishing clinically valid radiomic signatures.

ABBREVIATIONS: AUROC = area under the receiver operating characteristic curve; BED = biologic effective dose; BOT = beam-on time; GLDM = gray-level dependence matrix; GLSZM = gray-level size zone matrix; ML = machine learning; SHAP = Shapley additive explanations; SRS = stereotactic radiosurgery; TDR = treatment dose rate

Stereotactic radiosurgery (SRS) is essential in the management of AVMs, the most prevalent vascular malformations of the brain, and it is particularly valuable in small AVMs and the ones juxtaposed to eloquent cortical regions. With a prolonged therapeutic course and expanding SRS applications covering complex AVMs, obliteration rates have shifted recently[1,2] making their prediction increasingly challenging. In addition to the important influence dosimetry has on the prognosis of AVMs following SRS,[3-5] the duration of intermittent treatment is also tightly connected with ensuring conformal therapy.[6-8] The biologic effective dose (BED) measure has shown a notable association with tissue survival,[7,8] incorporating both radiation dosage and beam-on time (BOT). BED was found to be predictive of AVM obliteration following single-session SRS.[9]

Currently, establishing a definitive diagnosis of a brain AVM is typically provided using DSA, which is considered the reference standard for evaluating cerebral AVMs in SRS planning and obliteration follow-up, owing to its high spatiotemporal resolution and accurate reflection of the detailed lesion angioarchitecture.[10-12]

Received June 1, 2023; accepted after revision May 9, 2024.

From the Departments of Radiology (M.S.J., M.A.M., H.K., W.B.), and Neurological Surgery (C.L.N., C.S.G., B.E.P., W.B.), Mayo Clinic, Rochester, Minnesota; and Department of Computer and Information Science (M.S.J.), University of Pennsylvania, Philadelphia, Pennsylvania.

Please address correspondence to Mohamed Sobhi Jabal, MD, Mayo Clinic Rochester, Department of Radiology, 200 First St. SW, Rochester, MN 55905-0002; e-mail: m.sobhi.jabal.research@gmail.com; @SobhiJabal; @WBrinjikji; @MayoRadiology

Indicates article with online supplemental data.

http://dx.doi.org/10.3174/ajnr.A8351

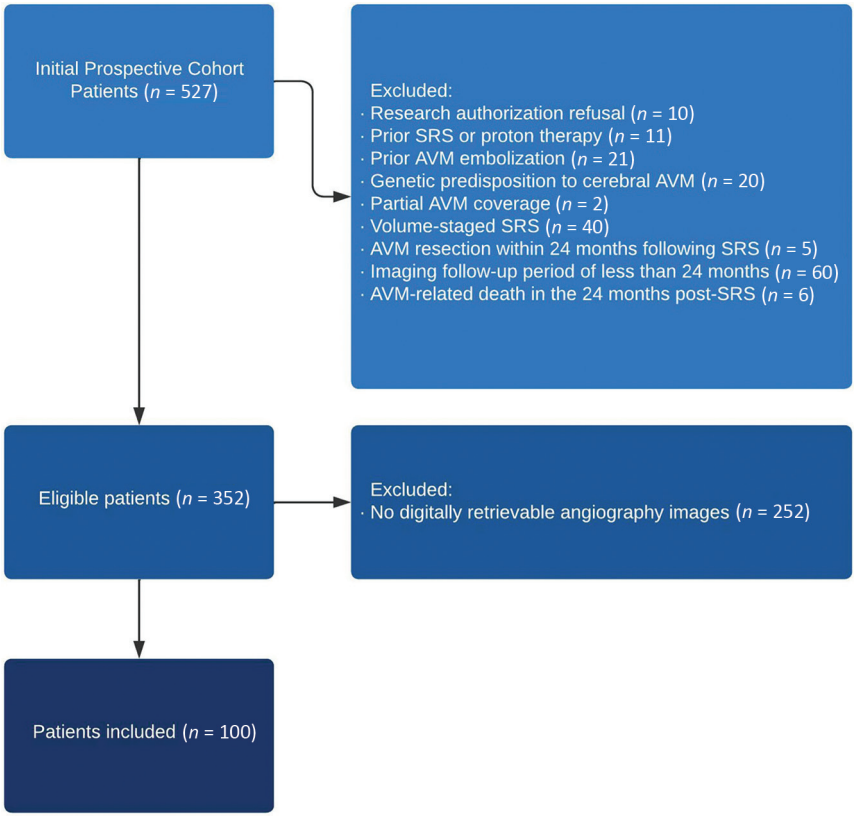

FIG 1. Flow diagram of patient inclusion and exclusion.

Radiomics-based applications, which use image processing and quantification of radiologic phenotypic lesion traits, are increasingly being used in the realm of precision medicine for diagnostic and prognostic tool development,[13-16] with a potential in biomarker analysis and clinical decision assistance,[17-19] overcoming some constraints inherent in subjective visual evaluation.[20] These techniques, capable of extracting molecular and pathophysiologic process data often imperceptible to the human eye, offer advantages over subjective visual evaluation.[21–22] The approach computes shape and textural information using spatial distribution of signal intensities and pixel interrelations, determined through mathematical formulas, thereby reducing subjective interreader variability and providing a good foundation for interpretable machine learning (ML) applications.[23,24]

Providing individualized predications of patient prognosis following SRS has valuable potential that is integral to the future of management of neurologic diseases. Numerous classical scoring systems have been developed to help clinicians better anticipate patient outcomes following radiosurgical management of brain AVMs.[25-32] In the present study, we aimed to develop a ML predictive approach to model extracted DSA radiomics features for brain AVM obliteration prediction following radiosurgery in comparison with clinical and radiosurgical predictors found in classical established scoring systems.

MATERIALS AND METHODS

Patients

This study was conducted through retrospective examination of an SRS cohort of 527 patients with cerebral AVMs between 1990 and 2014, registered prospectively. The scope was limited to patients who underwent single-session SRS using the Leksell Gamma Knife (EleKta) for sporadic AVMs, having baseline imaging and at least 2 years of angiography or MR imaging follow-up. A summary of the inclusion process is shown in Fig 1.[9] In total, of the eligible 352 patients, 100 patients had digitally retrievable angiography images and were included in the final analysis. The patients' clinical and radiosurgical characteristics were included, with the primary outcome being total AVM obliteration, defined as the lack of flow voids on MR imaging or the absence of aberrant arteriovenous shunting on angiography. A minimum of 2 years for imaging follow-up with either DSA or MR imaging was chosen to reflect the minimum expected time for post-SRS AVM obliteration. The study was approved by the Mayo Clinic institutional review board.

Clinical and Radiosurgical Features

Clinical and lesion characteristics included age, female sex, bleeding and/or seizure at presentation, lesion diameter, lesion volume, location, rupture status, prior resection, prior embolization, deep location, size, eloquent location, deep vein drainage, and the Spetzler-Martin grading scale. Radiosurgical features included the following: BED, maximum dose, margin dose, treatment time, treatment dose rate (TDR), isodose, and modified radiosurgery-based AVM score. The feature values were normalized to a range between 0 and 1.

Image Segmentation and Radiomics Feature Extraction

Patients' baseline DSA series were screened. 2D anterior-posterior and lateral view DSA images corresponding to SRS planning and with a peak arterial phase were selected. Lesion segmentation was performed using 3D Slicer software (http://www.slicer.org)[33,34] by an experienced radiologist with the guidance and supervision of an experienced interventional neuroradiologist. For each patient, 2 ROIs of the AVM lesion were delineated excluding the draining vein, from both the anterior-posterior and lateral DSA.

Following the segmentation, AVM radiomics features were computed using pyradiomics, Version 3.0.1,[35] with Python, Version 3.8. A total of 200 radiomics features (first-order, shape-based, and higher-order features) were extracted, 100 from each of the anterior-posterior view and lateral views of every patient's angiogram. The features were also scaled between 0 and 1 to facilitate the algorithm learning process. For dimensionality reduction of the radiomics variables, the maximum relevance minimum redundancy[36,37] method was implemented to select a reduced variable number of 20% of the feature space and retain the most important and least collinear information. Maximum relevance minimum redundancy was applied by fitting and transforming the training

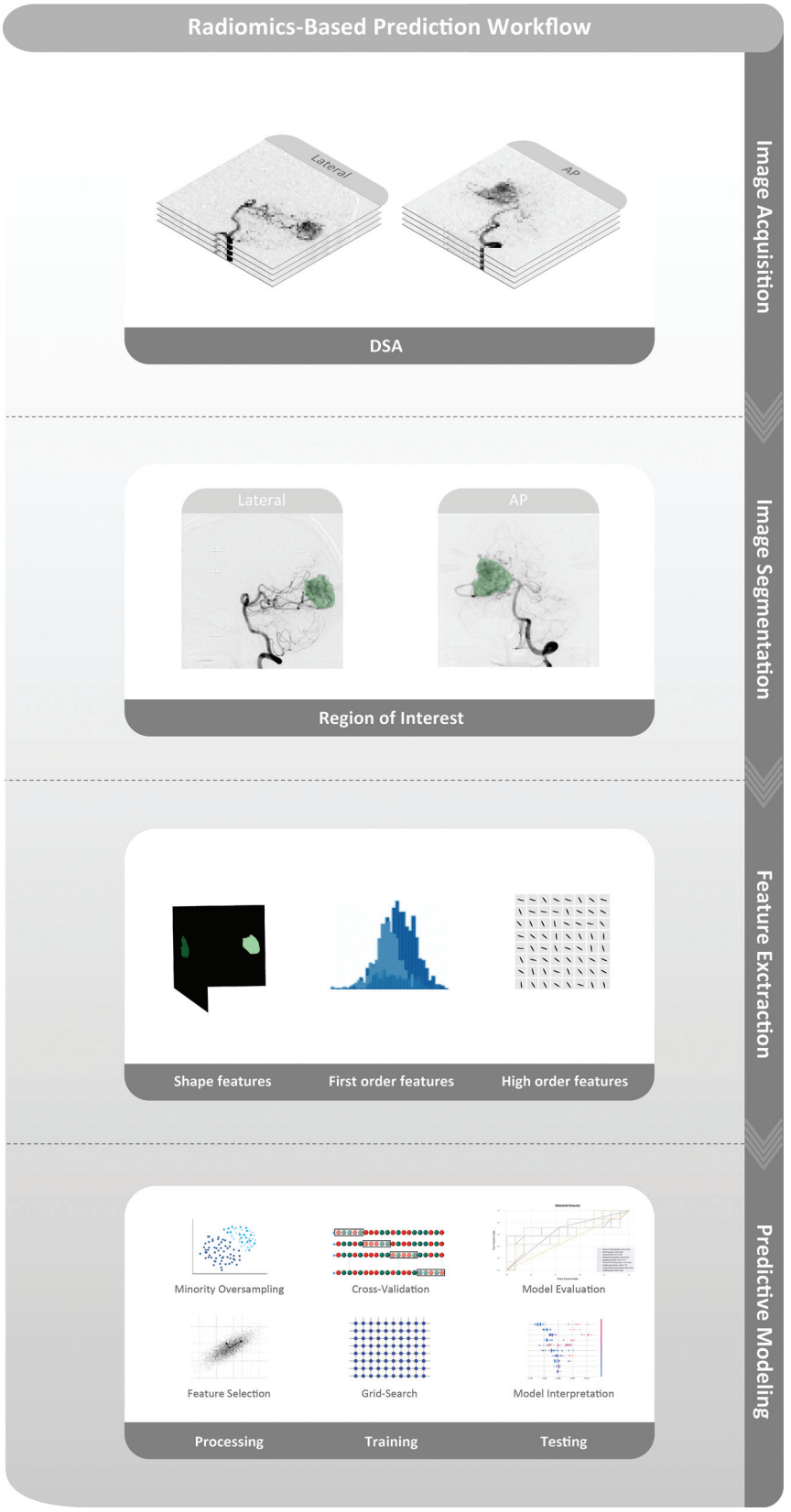

FIG 2. Workflow for DSA radiomics predictive modeling of cerebral AVM obliteration following SRS.

set and with no fitting and only transforming the test set to avoid any data leakage. An illustrative figure of the radiomics and prediction modeling workflow is demonstrated in Fig 2.

Statistical Analysis

Demographic and clinico-radiosurgical variables were statistically analyzed between the 2 patient outcome groups using SciPy (Version 1.6.2; https://scipy.org/) and Python. A univariate statistical comparison between the patient groups was performed regarding the obliteration outcome. Continuous quantitative variables were assessed given their distribution normality using the Student t test and Wilcoxon rank-sum test. The χ^2 test was used to compare the categoric variables. P values $< .05$ were considered statistically significant.

ML Modeling

ML models were constructed to predict unsuccessful AVM total obliteration. The synthetic minority oversampling technique CURE-SMOTE (https://bmcbioinformatics.biomedcentral.com/articles/10.1186/s12859-017-1578-z#abbreviations),[38] derivative of the synthetic minority over-sampling technique (SMOTE),[39] was deployed to artificially generate minority class data and correct the training set class imbalance. The stratified split of the data set into a training set of 80% and a test set of 20% was applied, after which 10-fold cross-validation was used on the training set. A grid search was used for hyperparameter tuning. The benchmarked models were the following: decision tree, Gaussian Naïve Bayes, multilayer perceptron, K-nearest neighbors, random forest, BaggingClassifier, gradient boosting classifier, and eXtreme Gradient Boosting (XGBoost; https://xgboost.readthedocs.io/en/stable/). Model performance was measured and compared across the ML algorithms.

Model Interpretation

Shapley additive explanations (SHAP), a game theory approach, was used to interpret the best-performing models by computing the contribution of each input feature to the prediction of an ML model and providing an importance ranking of contributing features.[40-42]

RESULTS

Patient Population and Data Set

The overall included cohort comprised 352 patients. Follow-up imaging had a median duration of 5.9 years following SRS and revealed obliteration in 259 patients (71.9%), verified by angiography in 176 (70%) patients and MR

imaging in 83 (30%) patients, occurring at a median interval of 36 months subsequent to SRS (interquartile range, 26–44 months). A total of 100 patients with cerebral AVMs and 200 images were included. The median patient age was 40.6 (SD, 16) years, with women representing 59% and patients with unsuccessful total obliteration representing 34% of the studied final data set. The selection process of the included cohort is summarized in Fig 1.

Statistical Analysis

Comparison of clinico-radiosurgical variables regarding cerebral AVM obliteration status following SRS is detailed in the Table. Statistical analysis indicated younger patients ($P = .02$), higher AVM volume ($P = .01$) and diameter ($P = .02$), and an increased number of isocenters used ($P = .004$) were significantly associated with failure of total AVM obliteration. While higher BED ($P = .002$), elevated maximal dose ($P = .002$) and margin dose, ($P = .002$) as well as a lower Spetzler Martin Scale grade ($P = .04$) had a statistically significant correlation with successful total AVM obliteration following SRS in the cohort.

ML Prediction and Interpretation

Following feature selection and cross-validation, evaluation of the developed ML models was performed on the test set. By means of the clinico-radiosurgical variables, the best performing model was a gradient boosting classifier with an area under the receiver operating characteristic curve (AUROC) of 68%, recall of 67%, and precision of 71%. Using radiomics variables, Adaptive Boosting (AdaBoost; https://www.machinelearningplus.com/machine-learning/introduction-to-adaboost/#google_vignette) had the best evaluation with an AUROC of 79%, recall of 75% and precision of 71%.

Figure 3 demonstrates the performance and evaluation metrics matrix comparison of predictive models for cerebral AVM obliteration following SRS using only clinical radiosurgical features (Fig 3*A*) in comparison with radiomics features (Fig 3*B*). SHAP summary plots (https://shap-lrjball.readthedocs.io/en/latest/generated/shap.summary_plot.html) in Fig 4*A*, *-D* depict the importance and impact direction of clinico-radiosurgical and radiomics features, respectively, on model predictions for obliteration failure. The color intensity represents a feature value, with SHAP values indicating the influence on the predictive outcome both in positive and negative correlations with the outcome. Heatmaps in Fig 4*B*, *-E* of the Shapley values for each feature across the instances in the test set demonstrate the individual contribution of clinico-radiosurgical and radiomics features to the predictions, with color gradients representing the magnitude of the impact. Bar charts in Fig 4*C*, *-F* illustrate the maximal impact of each clinico-

Univariate statistical comparison of the 2 patient groups relating to total obliteration status

Variable	All	Total Obliteration	No Total Obliteration	*P* Value
Age	43	45 (32–56)	38 (20–47)	.023
Sex				.850
Male	41	28 (42%)	13 (38%)	
Female	59	38 (58%)	21 (62%)	
Ruptured				.733
No	82	53 (80%)	29 (85%)	
Yes	18	13 (20%)	5 (15%)	
Prior resection				.571
No	93	61 (92%)	32 (94%)	
Resection	4	2 (3%)	2 (6%)	
Location				.288
Hemispheric	91	62 (94%)	29 (85%)	
Deep	9	4 (6%)	5 (15%)	
Eloquent				.363
No	37	27 (41%)	10 (29%)	
Yes	63	39 (59%)	24 (71%)	
Deep vein drainage				.219
No	57	41 (62%)	16 (47%)	
Yes	43	25 (38%)	18 (53%)	
Isocenters	6	6.0 (4,7)	7.0 (5,9)	.005
Volume (cm^3)	3.8	2.9 (1,6)	6.1 (2,8)	.016
Treatment time	48.24	46.805 (32–63)	50.665 (34–68)	.330
TDR	2.77	2.80 (2,3)	2.74 (2,3)	.346
BED	137	148 (115–173)	119 (104–147)	.003
Maximum dose	40	40.0 (36–44)	36.0 (36–40)	.002
Margin dose	20	20.0 (18–22)	18.0 (18–20)	.002

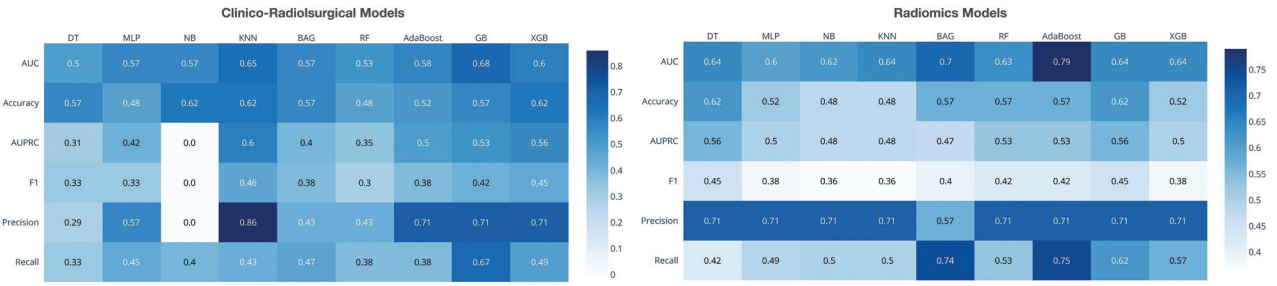

FIG 3. Performance evaluation metrics matrix of predictive models for cerebral AVM obliteration following SRS using only clinical radiosurgical features (*A*) in comparison with radiomics features (*B*).

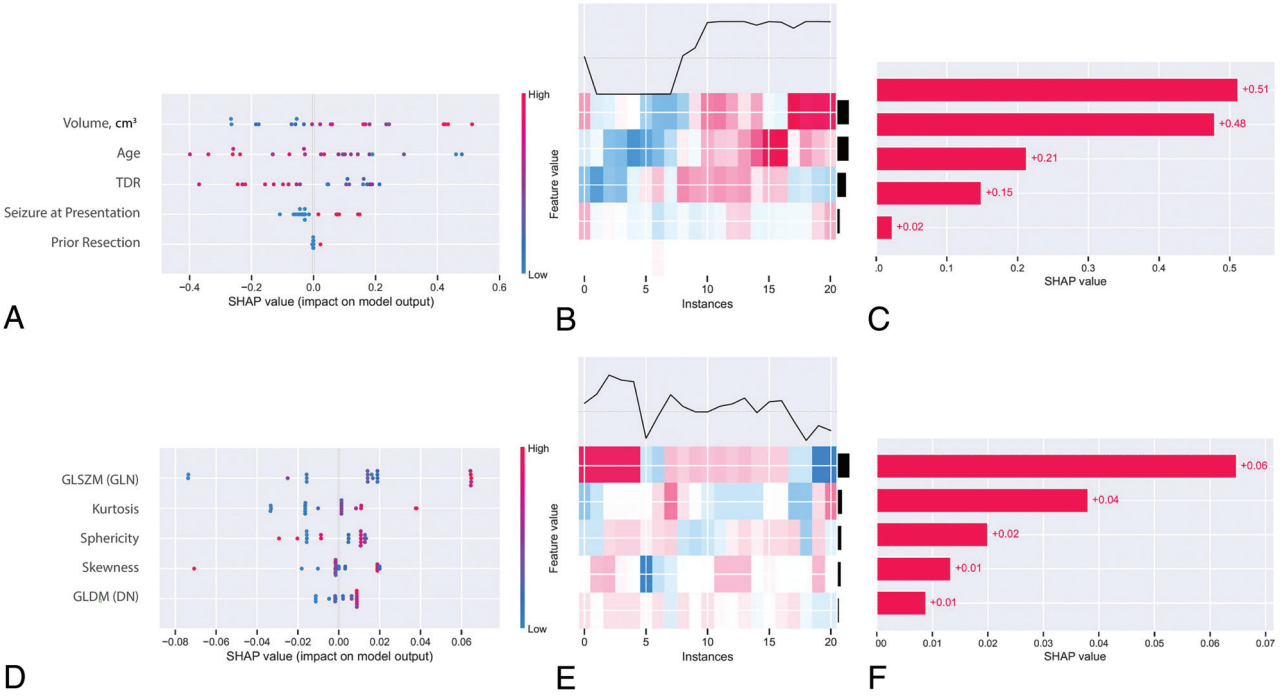

FIG 4. Interpretation of the best-performing clinico-radiosurgical (*A–C*) and radiomics (*D–F*) models including SHAP summary plots (*A* and *D*) with the colored test instances signifying feature value, SHAP heatmaps (*B* and *E*) where the red and blue refer to positive and negative SHAP values, and maximal feature SHAP bar plots (*C* and *F*) for the clinico-radiosurgical and radiomics models, respectively.

radiosurgical and radiomics feature on the outcome prediction of the model, ranked by their importance.

Global interpretation plots are represented in the Online Supplemental Data for the best-performing radiomics and clinico-radiosurgical models, demonstrating the overall prediction patterns across the test set according to obliteration outcomes. Local explanations for predictions of individual patients' successful and unsuccessful obliteration outcomes are illustrated in the Online Supplemental Data, showcasing the interplay of features for specific cases.

The ranked most important clinico-radiosurgical features were lesional volume, patient age, TDR, seizure at presentation, and prior resection. The ranked most important radiomics features were gray-level size zone matrix (GLSZM), gray-level nonuniformity, kurtosis, skewness, and gray-level dependence matrix (GLDM) dependence nonuniformity.

DISCUSSION

The study findings highlight the value of combining quantitative morphologic imaging features with ML for predicting post-2-year total obliteration of cerebral AVMs following SRS. Models built using radiomics features achieved better overall performance and higher sensitivity compared with those constructed with classic clinico-radiosurgical variables, and relevant clinical and radiosurgical variables. Model interpretation identified key variables like lesion volume, patient age, TDR, and prior resection as top contributors, validating their significance.

In the constructed radiomics model, GLSZM gray-level nonuniformity was the most important radiomics feature driving prediction, with greater values associated with a higher probability of unfavorable AVM obliteration. GLSZM gray-level nonuniformity informs the connectedness and variability of gray-level intensity values, with a lower value indicating homogeneous intensity. This feature underscores how highly compact nidi have a more favorable chance of total obliteration in post-2-year follow-up. Kurtosis, quantifying ROI intensity distribution with high values implying distribution concentration, is located at the tails rather than the center, inferring prevalence of extreme intensity values, which could also be characteristic of diffuse AVM. This finding is in line with previous studies on the topic.[43]

In a recent study by Gao et al,[44] radiomics models were developed to predict the outcomes of gamma knife radiosurgery for unruptured AVMs. However, unlike our study, which used lateral DSA views to capture radiomics features, Gao et al relied on cross-sectional MR imaging. The use of DSA in our study, recognized as the criterion standard due to its superior spatial resolution, allows a more precise analysis of AVM nidus architecture and could potentially provide more accurate predictive insight than MR-based imaging. This distinction is crucial because DSA provides dynamic vascular information that MRIs typically do not capture, possibly leading to better-tailored treatment plans based on more detailed vascular data.

GLDM describes how several connected pixels within a certain distance are dependent on the intensity of the center pixel. Dependence nonuniformity informs unequal dependence through the ROI, indicating heterogeneous dependencies, associated with unfavorable AVM obliteration outcome.

Skewness corresponds to the asymmetry of intensity value distribution around the mean, and sphericity quantifies the roundness of the ROI relative to a circle. Of note, all Maximum Relevance Minimum Redundancy–selected radiomics features originated from the lateral DSA view.

With results closely consistent with our clinico-radiosurgical model findings, Oermann et al[45] developed an ML approach using only clinico-radiosurgical features from a large cohort with a post-2-year obliteration prediction performance of 0.70. Meng et al[46] built a radiomics-based ML model to forecast cerebral AVM outcomes post-SRS following partial embolization using MR T2 images of 100 patients. Despite a K-nearest neighbors model AUROC of 0.66, its specificity of 0.44 was lower compared with their leading dosimetry model (AUROC = 0.66, specificity = 0.56). They suggested that the cohort's prior embolization, possibly causing lesion homogeneity, weakened the prognostic strength of the radiomics models. The model comprised 4 radiomics features: minor-axis-length, total energy, and 2 types of gray-level nonuniformity. Two studies used AVM radiomics for diagnosis with no prediction of outcomes: Jiao et al[47] used segmented 3D TOF-MRA images, and Shi et al[48] trained a neural network model for temporospatial diagnosis of AVMs from DSA sequences for dichotomized AVM grade classification.

The study design choice for prognostic models of SRS AVM obliteration using DSA, which is the criterion standard with high spatial resolution, as well as the exclusion of patients with prior AVM embolization have allowed highlighting predictive radiomics markers. We believe such models may provide a significant step toward enhanced prediction of AVM obliteration, and with further validation and refinement, they could support clinical decision-making processes. The current study shows the potential of ML and radiomics in automating the assessment of AVM features in a precise quantitative manner with the end goal of validating radiomics signatures for SRS outcome prediction. It also underlines the promise of future prognostic tools in personalized data-centered cerebrovascular care. Future studies should further explore the radiomics association with patient presentation characteristics, such as seizures.

Limitations

Although the sample size of this study is considered within the normal range for radiomics research,[49-51] size remains a limiting factor for reliable generalization of the findings, and future larger multicenter projects and prospective model implementation are recommended for further validation of features predictive of cerebral AVM obliteration. Similarly, the age of our cohort may be slightly greater than that in other published studies. We recommend implementing a nested cross-validation approach incorporating the feature selection in future studies with larger sample-size populations. Another limitation may relate to not examining the different DSA machine types and intra-arterial contrast injection approaches used and the existence of potential variability between them during the span of the study and how that might influence the extracted radiomic features.

CONCLUSIONS

The combination of ML methods and quantifiable image-based markers is a valuable approach to model cerebral AVM outcome managed with SRS and could complement classic prognostic tools. In this study, a radiomics-based ML model was built to predict AVM obliteration following radiosurgical treatment. In line with the prior knowledge in the field and bringing added precision to its assessment, the predictive findings might hypothetically be based on DSA features related to the diffuseness and angioarchitecture of AVMs, which need to be verified in future studies. Model interpretation has become an essential step of ML pipelines in health care to ensure the clinical soundness and validity of prognostic radiomic biomarkers.

Disclosure forms provided by the authors are available with the full text and PDF of this article at www.ajnr.org.

REFERENCES

1. Patibandla MR, Ding D, Kano H, et al. **Effect of treatment period on outcomes after stereotactic radiosurgery for brain arteriovenous malformations: an international multicenter study.** *J Neurosurg* 2018;130:579–88 CrossRef Medline
2. Pollock BE, Link MJ, Stafford SL, et al. **Stereotactic radiosurgery for arteriovenous malformations: the effect of treatment period on patient outcomes.** *Neurosurgery* 2016;78:499–509 CrossRef Medline
3. Ding D, Starke RM, Kano H, et al. **Radiosurgery for unruptured brain arteriovenous malformations: an international multicenter retrospective cohort study.** *Neurosurgery* 2017;80:888–98 CrossRef Medline
4. Flickinger JC, Pollock BE, Kondziolka D, et al. **A dose response analysis of arteriovenous malformation obliteration after radiosurgery.** *Int J Radiat Oncol Biol Phys* 1996;36:873–79 CrossRef Medline
5. Karlsson B, Lindquist C, Steiner L. **Prediction of obliteration after gamma knife surgery for cerebral arteriovenous malformations.** *Neurosurgery* 1997;40:425–30; discussion 430–21 CrossRef Medline
6. Hopewell JW, Millar WT, Lindquist C, et al. **Application of the concept of biologically effective dose (BED) to patients with vestibular Schwannomas treated by radiosurgery.** *J Radiosurg SBRT* 2013; 2:257–71 Medline
7. Jones B, Hopewell JW. **Modelling the influence of treatment time on the biological effectiveness of single radiosurgery treatments: derivation of "protective" dose modification factors**. *Br J Radiol* 2019;92:20180111 CrossRef Medline
8. Millar WT, Hopewell JW, Paddick I, et al. **The role of the concept of biologically effective dose (BED) in treatment planning in radiosurgery.** *Phys Med* 2015;31:627–33 CrossRef Medline
9. Nesvick CL, Graffeo CS, Brown PD, et al. **The role of biological effective dose in predicting obliteration after stereotactic radiosurgery of cerebral arteriovenous malformations.** *Mayo Clin Proc* 2021;96:1157–64 CrossRef Medline
10. Oppenheim C, Meder JF, Trystram D, et al. **Radiosurgery of cerebral arteriovenous malformations: is an early angiogram needed?** *AJNR Am J Neuroradiol* 1999;20:475–81 Medline
11. Steiner L, Lindquist C, Adler JR, et al. **Clinical outcome of radiosurgery for cerebral arteriovenous malformations.** *J Neurosurg* 1992; 77:1–8 CrossRef Medline
12. Derdeyn CP, Zipfel GJ, Albuquerque FC, et al; American Heart Association Stroke Council. **Management of brain arteriovenous malformations: a scientific statement for healthcare professionals from the American Heart Association/American Stroke Association.** *Stroke* 2017;48:e200–24 CrossRef Medline
13. Aerts HJ. **The Potential of Radiomic-Based Phenotyping in Precision Medicine: A Review.** *JAMA Oncol* 2016;2:1636–42 CrossRef Medline
14. Hassani C, Varghese BA, Nieva J, et al. **Radiomics in pulmonary lesion imaging.** *AJR Am J Roentgenol* 2019;212:497–504 CrossRef Medline
15. Han Y, Yang Y, Shi ZS, et al. **Distinguishing brain inflammation from grade II glioma in population without contrast enhancement: a radiomics analysis based on conventional MRI.** *Eur J Radiol* 2021; 134:109467 CrossRef Medline
16. Su Y, Xu X, Zuo P, et al. **Value of MR-based radiomics in differentiating uveal melanoma from other intraocular masses in adults.** *Eur J Radiol* 2020;131:109268 CrossRef Medline

17. Lambin P, Leijenaar RT, Deist TM, et al. **Radiomics: the bridge between medical imaging and personalized medicine.** *Nat Rev Clin Oncol* 2017;14:749–62 CrossRef Medline
18. Christie JR, Lang P, Zelko LM, et al. **Artificial intelligence in lung cancer: bridging the gap between computational power and clinical decision-making.** *Can Assoc Radiol J* 2021;72:86–97 CrossRef Medline
19. Bi WL, Hosny A, Schabath MB, et al. **Artificial intelligence in cancer imaging: clinical challenges and applications.** *CA Cancer J Clin* 2019;69:127–57 CrossRef Medline
20. Sala E, Mema E, Himoto Y, et al. **Unravelling tumour heterogeneity using next-generation imaging: radiomics, radiogenomics, and habitat imaging.** *Clin Radiol* 2017;72:3–10 CrossRef Medline
21. Neisius U, El-Rewaidy H, Nakamori S, et al. **Radiomic analysis of myocardial native T1 imaging discriminates between hypertensive heart disease and hypertrophic cardiomyopathy.** *JACC Cardiovasc Imaging* 2019;12:1946–54 CrossRef Medline
22. Mannil M, von Spiczak J, Manka R, et al. **Texture analysis and machine learning for detecting myocardial infarction in noncontrast low dose computed tomography: unveiling the invisible.** *Invest Radiol* 2018;53:338–43 CrossRef Medline
23. Castellano G, Bonilha L, Li LM, et al. **Texture analysis of medical images.** *Clin Radiol* 2004;59:1061–69 CrossRef Medline
24. Tourassi GD. **Journey toward computer-aided diagnosis: role of image texture analysis.** *Radiology* 1999;213:317–20 CrossRef Medline
25. Ding D, Liu KC. **Predictive capability of the Spetzler-Martin versus supplementary grading scale for microsurgical outcomes of cerebellar arteriovenous malformations.** *J Cerebrovasc Endovasc Neurosurg* 2013;15:307–10 CrossRef Medline
26. Pollock BE, Flickinger JC, Lunsford LD, et al. **Factors that predict the bleeding risk of cerebral arteriovenous malformations.** *Stroke* 1996;27:1–6 CrossRef Medline
27. Stapf C, Mast H, Sciacca RR, et al. **Predictors of hemorrhage in patients with untreated brain arteriovenous malformation.** *Neurology* 2006;66:1350–55 CrossRef Medline
28. Pollock BE, Flickinger JC. **Modification of the radiosurgery-based arteriovenous malformation grading system.** *Neurosurgery* 2008;63:239–43; discussion 243 CrossRef Medline
29. De Oliveira E, Tedeschi H, Raso J. **Comprehensive management of arteriovenous malformations.** *Neurol Res* 1998;20:673–83 CrossRef Medline
30. Wegner RE, Oysul K, Pollock BE, et al. **A modified radiosurgery-based arteriovenous malformation grading scale and its correlation with outcomes.** *Int J Rad Oncol Biol Phys* 2011;79:1147–50 CrossRef Medline
31. Lawton MT, Kim H, McCulloch CE, et al. **A supplementary grading scale for selecting patients with brain arteriovenous malformations for surgery.** *Neurosurgery* 2010;66:702–13; discussion 713 CrossRef Medline
32. Kim H, Abla AA, Nelson J, et al. **Validation of the supplemented Spetzler-Martin grading system for brain arteriovenous malformations in a multicenter cohort of 1009 surgical patients.** *Neurosurgery* 2015;76:25–33 CrossRef Medline
33. Fedorov A, Beichel R, Kalpathy-Cramer J, et al. **3D Slicer as an image computing platform for the Quantitative Imaging Network.** *Magn Reson Imaging* 2012;30:1323–41 CrossRef Medline
34. Pinter C, Lasso A, Fichtinger G. **Polymorph segmentation representation for medical image computing.** *Comput Methods Programs Biomed* 2019;171:19–26 CrossRef Medline
35. van Griethuysen JJM, Fedorov A, Parmar C, et al. **Computational radiomics system to decode the radiographic phenotype.** *Cancer Res* 2017;77:e104–07 CrossRef Medline
36. Ding C, Peng H. **Minimum redundancy feature selection from microarray gene expression data.** *J Bioinforma Comput Biol* 2005;03:185–205 CrossRef Medline
37. Peng H, Long F, Ding C. **Feature selection based on mutual information: criteria of max-dependency, max-relevance, and min-redundancy.** *IEEE Trans Pattern Anal Mach Intell* 2005;27:1226–38 CrossRef Medline
38. Ma L, Fan S. **CURE-SMOTE algorithm and hybrid algorithm for feature selection and parameter optimization based on random forests.** *BMC Bioinformatics* 2017;18:169 CrossRef Medline
39. Chawla NV, Bowyer KW, Hall LO, et al. **SMOTE: synthetic minority over-sampling technique.** *Journal of Artificial Intelligence Research* 2002;16:321–57 CrossRef
40. Lundberg SM, Allen PG, Lee SI. **A unified approach to interpreting model predictions. advances in neural information processing systems. November 2017.** *arXiv*:1705.07874 [cs.AI] http://arxiv.org/abs/1705.07874. Accessed May 1, 2023
41. Lundberg SM, Nair B, Vavilala MS, et al. **Explainable machine-learning predictions for the prevention of hypoxaemia during surgery.** *Nat Biomed Eng* 2018;2:749–60 CrossRef Medline
42. Lundberg SM, Erion G, Chen H, et al. **From local explanations to global understanding with explainable AI for trees.** *Nat Mach Intell* 2020;2:56–67 CrossRef Medline
43. Yang HC, Peng SJ, Lee CC, et al. **Does the diffuseness of the nidus affect the outcome of stereotactic radiosurgery in patients with unruptured cerebral arteriovenous malformations?** *Stereotact Funct Neurosurg* 2021;99:113–22 CrossRef Medline
44. Gao D, Meng X, Jin H, et al. **Assessment of gamma knife radiosurgery for unruptured cerebral arteriovenous malformations based on multi-parameter radiomics of MRI.** *Magn Reson Imaging* 2022;92:251–59 CrossRef Medline
45. Oermann E, Rubinsteyn A, Ding D, et al. **Using a machine learning approach to predict outcomes after radiosurgery for cerebral arteriovenous malformations.** *Sci Rep* 2016;6:21161 CrossRef Medline
46. Meng X, Gao D, He H, et al. **A machine learning model predicts the outcome of SRS for residual arteriovenous malformations after partial embolization: a real-world clinical obstacle.** *World Neurosurg* 2022;163:e73–82 CrossRef Medline
47. Jiao Y, Zhang JZ, Zhao Q, et al. **Machine learning-enabled determination of diffuseness of brain arteriovenous malformations from magnetic resonance angiography.** *Transl Stroke Res* 2021;13:939–48 CrossRef Medline
48. Shi K, Xiao W, Wu G, et al. **Temporal-spatial feature extraction of DSA video and its application in AVM diagnosis.** *Front Neurol* 2021;12:655523 CrossRef Medline
49. Kleinbaum DG, Kupper LL, Muller KE, eds. *Applied Regression Analysis and Other Multivariable Methods*. Boston: PWS Kent Publishing Co; 1988
50. Sollini M, Cozzi L, Antunovic L, et al. **PET radiomics in NSCLC: state of the art and a proposal for harmonization of methodology.** *Sci Rep* 2017;7:358 CrossRef Medline
51. Gillies RJ, Kinahan PE, Hricak H. **Radiomics: images are more than pictures, they are data.** *Radiology* 2016;278:563–77 CrossRef Medline